RAA 2015 Vol. **15** No. **3**, 393–406 doi: 10.1088/1674–4527/15/3/008
http://www.raa-journal.org *http://www.iop.org/journals/raa*

Research in Astronomy and Astrophysics

Kinematics of solar neighborhood stars and its dependence on age and metallicity *

Zong-Bo Huyan, Zi Zhu and Jia-Cheng Liu

School of Astronomy and Space Science, Nanjing University, Nanjing 210093, China; *huyanzongbo@hotmail.com*
Key Laboratory of Modern Astronomy and Astrophysics, Ministry of Education (Nanjing University), Nanjing 210093, China

Received 2014 January 7; accepted 2014 May 21

Abstract We have constructed a catalog containing the best available astrometric, photometric, radial velocity and astrophysical data for mainly F-type and G-type stars (called the Astrometric Catalog associated with Astrophysical Data, ACAD). This contains 27 553 records and is used for the purpose of analyzing stellar kinematics in the solar neighborhood. Using the Lindblad-Oort model and compiled ACAD, we calculated the solar motion and Oort constants in different age–metallicity bins. The evolution of kinematical parameters with stellar age and metallicity was investigated directly. The results show that the component of the solar motion in the direction of Galactic rotation (denoted S_2) linearly increases with age, which may be a consequence of the scattering processes, and its value for a dynamical cold disk was found to be 8.0 ± 1.2 km s^{-1}. S_2 also linearly increases with metallicity, which indicates that radial migration is correlated to the metallicity gradient. On the other hand, the rotational velocity of the Sun around the Galactic center has no clear correlation with ages or metallicities of stars used in the estimation.

Key words: catalogs — solar neighborhood — Galaxy: kinematics and dynamics — Galaxy: evolution

1 INTRODUCTION

Positions, velocities, ages and chemical compositions of stars in the solar neighborhood are fundamental data for testing the models of local Galactic kinematics and evolution. Therefore, a comprehensive catalog with all these stellar parameters is necessary for the purpose of studying our Galaxy.

Since the Hipparcos catalog has provided high-precision three-dimensional positions and proper motions for nearby stars, radial velocities turn out to be important supplementary material for more accurately estimating Galactic kinematics. In the last ten years, some new radial velocity data were obtained and some old radial velocity data were improved. Gontcharov (2006) built the Pulkovo Compilation of Radial Velocities (PCRV) which contains weighted mean radial velocities for 35 495 Hipparcos stars. The Radial Velocity Experiment (RAVE), a milestone survey aiming at measuring the radial velocity of stars in the thick disk, was constructed by Steinmetz et al. (2006) and the catalog

* Supported by the National Natural Science Foundation of China.

has been updated to its third version (Siebert et al. 2011). Ages and metallicities, used to estimate the evolution of stars, are also important. Several catalogs with astrophysical data have been presented since the 1990s. Considering that a number of kinematical analyses of K and M giants have been performed (e.g. Miyamoto & Soma 1993, Famaey et al. 2005), we focused on collecting F-type and G-type stars in the solar neighborhood.

A very important work on kinematical evolution by Dehnen & Binney (1998) studied the relationship between stellar kinematics and velocity dispersions/colors based on the Hipparcos proper motions. It showed that the solar motion along the direction of Galactic rotation (denoted S_2) is related to the ages of the stars which form the local standard of rest (LSR). We mention that no radial velocity data were used in that work and the method of estimation is more or less indirect.

In Section 2, we collect the best current astrometric data, radial velocities and astrophysical data of F-type and G-type stars to construct a comprehensive catalog, called the Astrometric Catalog associated with Astrophysical Data (ACAD). In Section 3, the Galactic kinematics are studied with the Lindblad–Oort model using various stellar parameters in ACAD. Then, in Section 4, we obtain relations between kinematics and age–metallicity and compare our results with previous works. Discussion and conclusions are provided in Section 5.

2 CATALOG COMPILATION

We compiled our catalog (ACAD) based on the following three main catalogs for F- and G-type stars:

- The Geneva–Copenhagen Survey of the solar neighborhood (GCS, Nordström et al. 2004). GCS aimed at consolidating the calibrations of $uvby$ photometry into distance, metallicity and age for F-type and G-type stars. Radial velocities in GCS are mainly provided by using the CORAVEL observations and were standardized to the IAU or Wilson velocity system.
- The catalog of ages, metallicities, orbital elements and other parameters for nearby F-type stars (Marsakov & Shevelev 1995, denoted MS95). MS95 contains metallicities for all the 5498 stars and ages for 3405 slightly evolved stars. However, the space velocities relative to the Sun are only available for 1787 stars.
- The N2K Consortium IV including new temperatures and metallicities for more than 100 000 FGK dwarfs (Ammons et al. 2006, denoted AM06). AM06 used a uniform procedure to estimate fundamental stellar properties of Tycho-2 stars (Høg et al. 2000). However, radial velocity and age data were not included in AM06.

By setting $0.1''$ as the upper limit on the separation of the spherical position for a common star, we cross-identified stars in the above three catalogs. We found that MS95 has no entries in common with the other two catalogs, while AM06 and GCS have fewer than 100 stars in common. For these stars, we used the GCS data because no age data were available in AM06 and the age/metallicity data in GCS were more accurate. The combined catalog (by cross-identification) of these three individual catalogs was the basis of our catalog.

However, this preliminary combined catalog still needs revisions and supplements to become the final version of the catalog for the following reasons. First, since the distances of stars in the three original catalogs are derived from photometric data, the results depend on different models and measurements of colors. Therefore, distances from the three catalogs are not consistent: they need to be revised in order to improve the accuracy and reliability. Second, radial velocities for almost half of the stars are not available from the three catalogs. In addition, updates to the current radial velocities are necessary for better accuracy. Finally, photometric data should be supplemented to determine the probable position of stars on the Hertzsprung–Russell diagram. In order to accomplish all these revisions and supplements, the same standard ($0.1''$ match radius criterion) was used whenever cross-identification was applied to find stars that are common in different catalogs.

2.1 Improve the Distance Data

The distances of stars in MS95 are photometric distances derived from absolute magnitudes based on Crawford (1975), Olsen (1984) and visual magnitudes. The absolute magnitudes and distances in GCS were obtained with a similar method as MS95. The uncertainty of photometric distance in GCS is around 13%. AM06 is a catalog built on the Tycho-2 (Høg et al. 2000) system. Ammons et al. (2006) estimated the distances for all the stars in Tycho-2 with the relation fitted from parallaxes, colors and proper motions in the Hipparcos catalog and the average error of the distances in AM06 is about 100%.

Since the accuracy of the Hipparcos parallaxes is better than most of the distance data in the three basic catalogs, the parallaxes from the Hipparcos catalog can be used to improve the accuracy. The distance data in the combined catalog were replaced with Hipparcos measurements if (1) the error of Hipparcos parallax is smaller than 25%, and (2) the error is smaller than 3 mas. Note that the distances in the three basic catalogs are either fitted from the Hipparcos catalog or have no color-dependent bias from Hipparcos parallaxes (Nordström et al. 2004), and all the distances are consistent with the Hipparcos system.

2.2 Supplementary Radial Velocities

Including three-dimensional velocities is one of the important features of our catalog, ACAD. For radial velocity data, we should make sure that no systematic differences exist between various input data. In our compilation, the following three catalogs were selected to supplement the radial velocities.

- The General Catalog of Radial Velocities (GCRV, Barbier-Brossat & Figon 2000). The radial velocities are derived from spectra and standardized to the IAU or Wilson velocity systems.
- Pulkovo radial velocities for 35 493 Hipparcos stars (PCRV, Gontcharov 2006). PCRV is a compilation from 203 publications. 12 are major catalogs which provide most (80%) of the data in PCRV. The GCRV is one of the 12 major catalogs: some stars in GCRV are used as a standard for adjusting the radial velocities in PCRV in the framework of the IAU standard.
- The third release of the Radial Velocity Experiment (RAVEIII, Siebert et al. 2011), which is focused on an area away from the plane of the Milky Way ($|b| > 25^\circ$) and on stars with apparent magnitudes $9 < I_{\rm DENIS} < 13$. The mean error of its radial velocities is $\sim 2\ {\rm km\ s^{-1}}$.

All the radial velocities provided by the above catalogs are adjusted to the IAU standard system with high precision; therefore, they are homogeneous and self-consistent. For stars that are identified as common from cross-identification, the source of radial velocity data was chosen by the priority order defined by GCRV, PCRV and RAVEIII. All the possibilities for space velocity are shown in Table 1. The positions and proper motions for all the stars from various catalogs are in the Hipparcos or Tycho-2 systems, which are also known as the International Celestial Reference Frame (ICRF) in optical bandpass. We can conclude that the six-dimensional space velocity data (including five astrometric parameters and one radial velocity) in the final catalog are systematically homogeneous.

Table 1 Statistics of Space Velocity Data in ACAD

Index	Proper motion	Radial velocity	Number
1	HIP	PCRV	233
2	HIP	GCS	10 453
3	HIP	GCRV	554
4	MS95	MS95	1787
5	HIP	RAVE	40
6	TYCHO-2	RAVE	14 486

2.3 Photometric Data in ACAD

The absolute magnitude and spectral type were also provided in ACAD. For the stars recognized as Hipparcos stars, we derived the absolute magnitude from the Hipparcos parallax and Hp magnitude (visual magnitude in Hipparcos system). For the rest, the original absolute magnitudes from the MS95 and GCS catalogs of stars were used, while for AM06 stars Tycho V magnitudes were used in computing the absolute magnitude with distance data.

The collected spectral type in ACAD was described by MK classification. The spectral type is composed of two parts: temperature class as an indication of the surface temperature and luminosity class as an indication of surface gravity. For stars without spectral type in the combined catalog, the Tycho-2 Spectral Type catalog (SpType) by Wright et al. (2003) was used as a supplement.

2.4 Age and Metallicity

GCS has been updated twice to GCSIII (Holmberg et al. 2009) and metallicities were re-calibrated by using the infrared flux method (Casagrande et al. 2011). However, we prefer to use GCS in this version for the following two reasons: (1) GCS is consistent with several previous works (e.g. Edvardsson et al. 1993) and has proven to be reliable enough. The GSCIII catalog needs to be further re-checked with independent methods for calculating age and metallicity before being applied as a part of ACAD: this will be done in the near future for the next version of ACAD. (2) The differences shown by age–metallicity between GCS and GCSIII are not very significant; the largest change in ages is only $\sim 10\%$. For most analyses of the kinematical evolution, this would not systematically affect the results.

2.5 Statistics of ACAD

ACAD is a combination of eight different catalogs (three basic catalogs for F-type and G-type stars, the Hipparcos catalog for the revision of distances, three radial velocity catalogs for supplements to and revisions of space velocity and one catalog for a supplement to spectral type). All the stars are filled with distance, space velocity and at least one type of astrophysical datum (age or metallicity). For all the spectra, about 23% are G-type, 75% are F-type and the rest are K-type or A-type. The distribution of the ACAD stars is plotted in Figure 1. The high-density regions with a Galactic latitude from -60° to -20° and from 20° to 60° are covered by RAVE, which targeted the thick disk. There are 27 553 stars in total and the statistics of different parameters are listed in Table 2.

Table 2 Statistics of different parameters of stars in ACAD

Description of data	Number
Total number of ACAD stars	27 553
Stars with absolute magnitude	27 553
Stars with spectral type	9443
Stars with space velocities	27 553
Stars with distances & space velocities & ages	12 464
Stars with distances & space velocities & [Fe/H]	27 553

The distances of all the stars in ACAD range from 1.3 to 446.4 pc, and 84.6% are within 100 pc. The youngest star in ACAD is 0.2 Gyr old and the oldest is 17.0 Gyr. Over 60% of ACAD stars are younger than the Sun (4.6 ± 0.1 Gyr, Bonanno et al. 2002) and almost half of the stars are between 1 and 3 Gyr old. The metallicities range from -3.2 [Sun] to 3.5 [Sun] and are centered at 0 [Sun] (the metallicity of the Sun).

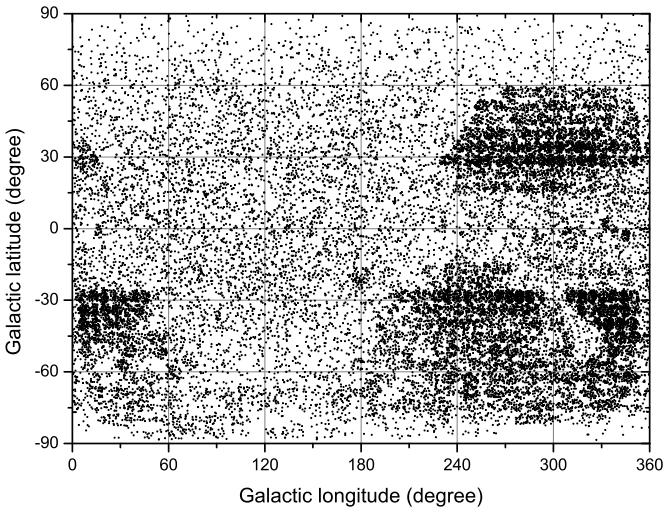

Fig. 1 The distribution of 27 553 ACAD stars in the Galactic coordinate system.

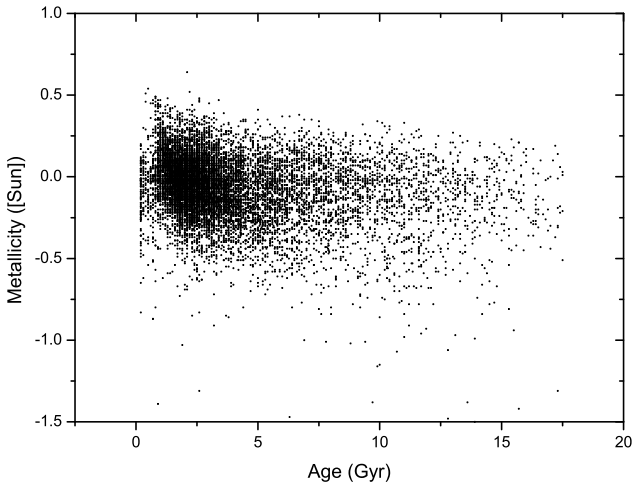

Fig. 2 Metallicity versus age for ACAD stars.

Figure 2 is the correlation of age and metallicity in ACAD, which shows that the two parameters are not obviously related. In the following sections, we will study the kinematical properties of stars in the solar neighborhood by using a sample selected from ACAD.

3 KINEMATICAL MODELS

To describe the characteristics of stellar motion in our Galaxy, it is practical to introduce the Galactocentric cylindrical coordinate system ($R,\ \theta,\ z$) where R is the radius from the Galactic center, θ the azimuthal angle measured from the axis directed to the Galactic center from the Sun,

and z the distance to the Galactic plane. Accordingly, we have V_R (the radial velocity with respect to the Galactic center), V_θ (the rotation projected onto the Galactic plane) and V_z (the velocity perpendicular to the Galactic plane). However, neither the velocity $\boldsymbol{V}(V_R, V_\theta, V_z)$ nor the position (R, θ, z) can be obtained directly from ACAD because all the measurements are expressed with respect to the Sun. It is necessary to establish a connection between the Galactocentric cylindrical coordinate system and the heliocentric Galactic coordinate system. The velocity field (V_R, V_θ, V_z) can be expanded in the Galactocentric cylindrical coordinate system as follows

$$\begin{pmatrix} V_R \\ V_\theta \\ V_z \end{pmatrix} = \begin{pmatrix} V_{R_\odot} \\ V_{\theta_\odot} \\ V_{z_\odot} \end{pmatrix} - \begin{pmatrix} S_1 \\ S_2 \\ S_3 \end{pmatrix} + \boldsymbol{M} \begin{pmatrix} \delta R \\ \delta\theta \\ \delta z \end{pmatrix}, \tag{1}$$

where $\boldsymbol{V}_\odot = (V_{R_\odot}, V_{\theta_\odot}, V_{z_\odot})^{\mathrm{T}}$ is the solar velocity in the Galactocentric cylindrical coordinate system; $\boldsymbol{S} = (S_1, S_2, S_3)$ is the solar motion with respect to the LSR. The matrix $\boldsymbol{M}$ is defined such that

$$\boldsymbol{M} = \boldsymbol{M}^+ + \boldsymbol{M}^-, \tag{2}$$

where $\boldsymbol{M}^-$ is a matrix representing the average angular velocity of all the stars moving as if they were a single rigid body. Ω_3 (equal to Oort constant A) is the angular velocity around the Galactic pole (z direction), which is more significant than the other two components perpendicular to the z axis (Zhu 2000; Miyamoto & Soma 1993). $\boldsymbol{M}^-$ can be written as

$$\boldsymbol{M}^- = \begin{pmatrix} 0 & -\Omega_3 & \Omega_2 \\ \Omega_3 & 0 & -\Omega_1 \\ -\Omega_2 & \Omega_1 & 0 \end{pmatrix}. \tag{3}$$

$\boldsymbol{M}^+$ is a symmetric matrix characterizing the deformation (oblique shear and dilatation) of the velocity field

$$\boldsymbol{M}^+ = \begin{pmatrix} M_{11}^+ & M_{12}^+ & M_{13}^+ \\ M_{12}^+ & M_{22}^+ & M_{32}^+ \\ M_{13}^+ & M_{32}^+ & M_{33}^+ \end{pmatrix}. \tag{4}$$

Specifically, the oblique shear is given by M_{ij}^+ $(i \neq j; i, j = 1, 2, 3)$. M_{12}^+ is the oblique shear on the Galactic plane which is much larger than the oblique shears on the other two planes perpendicular to the Galactic plane. M_{12}^+ is also known as the Oort constant B. The details of the above equations can be found in Zhu (2000) and Miyamoto & Soma (1993).

We note that only $(V_r, V_\ell, V_b)^{\mathrm{T}}$ and $(r, \ell, b)^{\mathrm{T}}$ measured in the heliocentric Galactic coordinate system are available; $\delta\boldsymbol{V} = \boldsymbol{V} - \boldsymbol{V}_\odot$ and $(\delta R, \delta\theta, \delta z)^{\mathrm{T}}$ should be transformed from $(V_r, V_\ell, V_b)^{\mathrm{T}}$ and $(r, \ell, b)^{\mathrm{T}}$. Then the 12 kinematical parameters can be solved with Equation (1). Because Ω_1, Ω_2, M_{32}^+, M_{33}^+, M_{22}^+, M_{13}^+ and M_{11}^+ are almost zero for a disk Galaxy (Zhu 2000; Miyamoto & Soma 1993), only $S_1,\ S_2,\ S_3$ and Oort constants A and B have significant values. This means that the stars in the solar neighborhood mainly move in the direction of Galactic rotation on the Galactic plane and the Galaxy does not notably expand in the radial direction. To restrict our model to these five main parameters, we use the two-demensional Lindblad–Oort model (on the Galactic plane)

$$\kappa\mu_\ell \cos b = S_1 \sin\ell/r - S_2 \cos\ell/r + \Omega_3 \cos b + M_{12}^+ \cos b \cos 2\ell\,, \tag{5}$$

$$V_r/r = -S_1 \cos\ell \cos b/r - S_2 \sin\ell \cos b/r - S_3 \sin b/r + M_{12}^+ \cos^2 b \sin 2\ell\,, \tag{6}$$

where $\kappa = 4.74047$ if the proper motion is given in the unit $\mathrm{mas\ yr^{-1}}$, the distance is in kpc and the velocity in $\mathrm{km\ s^{-1}}$. μ_ℓ is the proper motion in Galactic longitude. Based on the simplified Lindblad–Oort model, we obtain the solar motion and Oort constants by a least-squares fit.

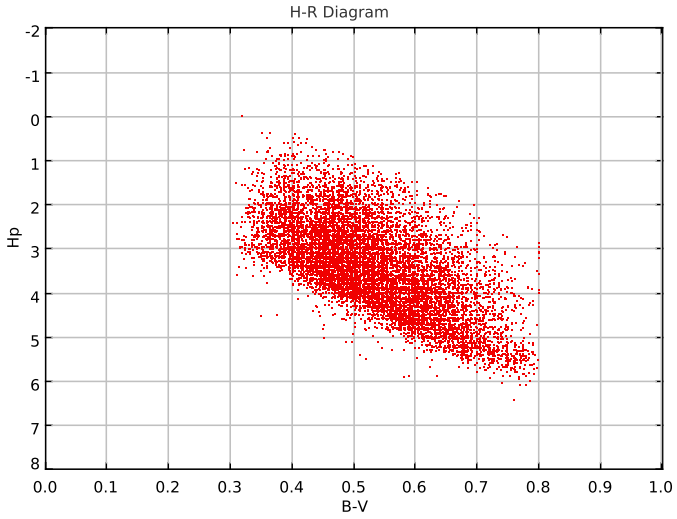

Fig. 3 The selected sample stars in the Hertzsprung-Russell diagram; the color index $B-V$ is restricted in [0.3, 0.8].

4 KINEMATICAL FEATURES DEPEND ON AGE AND METALLICITY

4.1 Selection of Samples from ACAD

The astrometric parameters (positions, distance and proper motions) and radial velocities are tied to the Hipparcos system and IAU standard, respectively; therefore, the parameters of stellar motion are homogeneous in ACAD. On the other hand, we should select stars with distance and radial velocity data which are accurate enough. Hence, the stars revised with Hipparcos parallaxes are selected. Another important principle in selecting sample stars is that they must be main-sequence stars so that they can meet the one-to-one relation between color and absolute luminosity. We applied a method similar to what was used by Dehnen & Binney (1998) to select the main-sequence stars with color range $0.3 < B-V < 0.8$. The selected stars are plotted on the Hertzsprung–Russell diagram in Figure 3. Selecting the stars in the thin disk is the third goal. Since the Sun is in the thin disk and the kinematical properties of the thin disk and the thick disk are different, stars in the solar neighborhood would be estimated more accurately with the LSR formed by thin disk stars. Schönrich & Binney (2009b) found that most of the thin disk stars are younger than 6.5 Gyr. We note that the number of young stars is too small for kinematical analysis; therefore, the upper limit of ages was set to be 6.5 Gyr and the lower limit was 1.5 Gyr. After these three steps of selection are applied, 7810 thin disk main-sequence stars are retained for the following analysis.

4.2 Kinematical Features of the Sample Stars

4.2.1 The evolution of solar motion and Oort constants A and B with age

In order to analyze the evolution of the kinematics, the sample stars are divided into several subsamples by age. We note that too few divisions cannot show a clear trend between kinematical parameters and age, but too many divisions would cause insufficient data in each subsample. After a few tests

Table 3 Kinematical parameters in different age bins for selected F-type and G-type stars in the ACAD catalog. The parameters derived from the K-M giants and F3-type stars are also listed for comparison.

	Unit	Min in all age bins	Max in all age bins	K-M giants	F3 stars
S_1		4.2 ± 1.2	7.7 ± 1.5	13.6 ± 0.3	11.4 ± 0.7
S_2	($\mathrm{km\ s^{-1}}$)	11.6 ± 0.5	16.7 ± 1.8	23.2 ± 0.3	14.1 ± 0.7
S_3		6.9 ± 0.8	10.9 ± 1.3	11.9 ± 0.3	8.7 ± 0.2
A	($\mathrm{km\ s^{-1}\ kpc^{-1}}$)	8.4 ± 0.6	14.3 ± 0.9	12.0 ± 0.6	13.8 ± 3.5
B		-20.7 ± 0.8	-7.8 ± 1.9	-8.6 ± 0.5	-12.7 ± 2.6

Notes: The K-M giants are distributed from 0.5 kpc to 1 kpc. F3-type stars are distributed from 0.1 kpc to 1.3 kpc (Miyamoto & Soma 1993).

and comparisons, a compromise scheme was used. We divided the sample stars between 1.5 and 6.5 Gyr into five groups with a bin of 1 Gyr.

Table 3 lists the variations of kinematical parameters in different age bins obtained from the least-squares fit to Equations (5) and (6); also listed are the values derived from K-M giants and F3-type stars (Miyamoto & Soma 1993).

In Figure 4, we plot the solar motion and Oort constants derived from the stars in each age bin. S_1, S_3 and Oort constants A and B have no systematical variation with respect to age. However, we found an obvious linear increase of S_2 with age by $1.8\ \mathrm{km\ s^{-1}\ Gyr^{-1}}$. This can be explained by the theory that scattering processes cause the random velocities of stars to steadily increase with age (Jenkins 1992). We also obtained $S_2 = 8.0 \pm 1.2\ \mathrm{km\ s^{-1}}$ by extrapolating the relation back to an age of 0 Gyr.

With the relation between velocity dispersion and solar motion, Dehnen & Binney (1998) found $S_2 = 5.3\ \mathrm{km\ s^{-1}}$ for a dynamical cold disk. However, Binney (2010) stated that the observed velocity distribution would be better fitted to the standard distribution function if the velocity dispersion could be shifted a little higher. This phenomenon implied that S_2 might be underestimated. By calculating the amount ($\delta S_2 = 5.8\ \mathrm{km\ s^{-1}}$) which should be added to S_2, $11.0\ \mathrm{km\ s^{-1}}$ should be a more realistic value for S_2.

The S_2 parameter for the dynamical cold disk in the former studies (e.g. Dehnen & Binney 1998) was based on the linear correlation between the squared velocity dispersion and solar motion. However, this linear correlation was based on the assumption that Galactic potential is axisymmetric. In reality, the amplitude of the non-axisymmetric potential effect on S_2 is about $7\ \mathrm{km\ s^{-1}}$. In our study, we fitted the correlation between solar motion and age more directly, which shows the evolution of solar motion with time.

Our result is larger than the result of Dehnen & Binney (1998) and the difference is smaller than the amplitude of the non-axisymmetric component. It demonstrates that $S_2 = 5.3\ \mathrm{km\ s^{-1}}$ is an underestimation by Dehnen & Binney (1998). At the same time, our result is smaller than that of Aumer & Binney (2009). The possible reason is the effect of spiral arm structure (which should be reduced) in the analysis. Although our sample stars are quite close to the Sun (within 450 pc) and are distributed uniformly in space, we cannot find an effective way to remove the influence of spiral structure. This effect makes the relationship between S_2 and age not strictly linear, so that S_2 for the dynamical cold disk is still underestimated. More data are needed to analyze the effect of the spiral structure on the local velocity field and to obtain the relation between solar motion and age more precisely.

4.3 The Variation of Solar Motion and Oort Constants A and B with Metallicity

The same procedure of grouping has been applied to analyzing the changes of kinematical parameters with metallicity. We divided the sample into five groups with a 0.2 [Sun] bin. As for the metal-

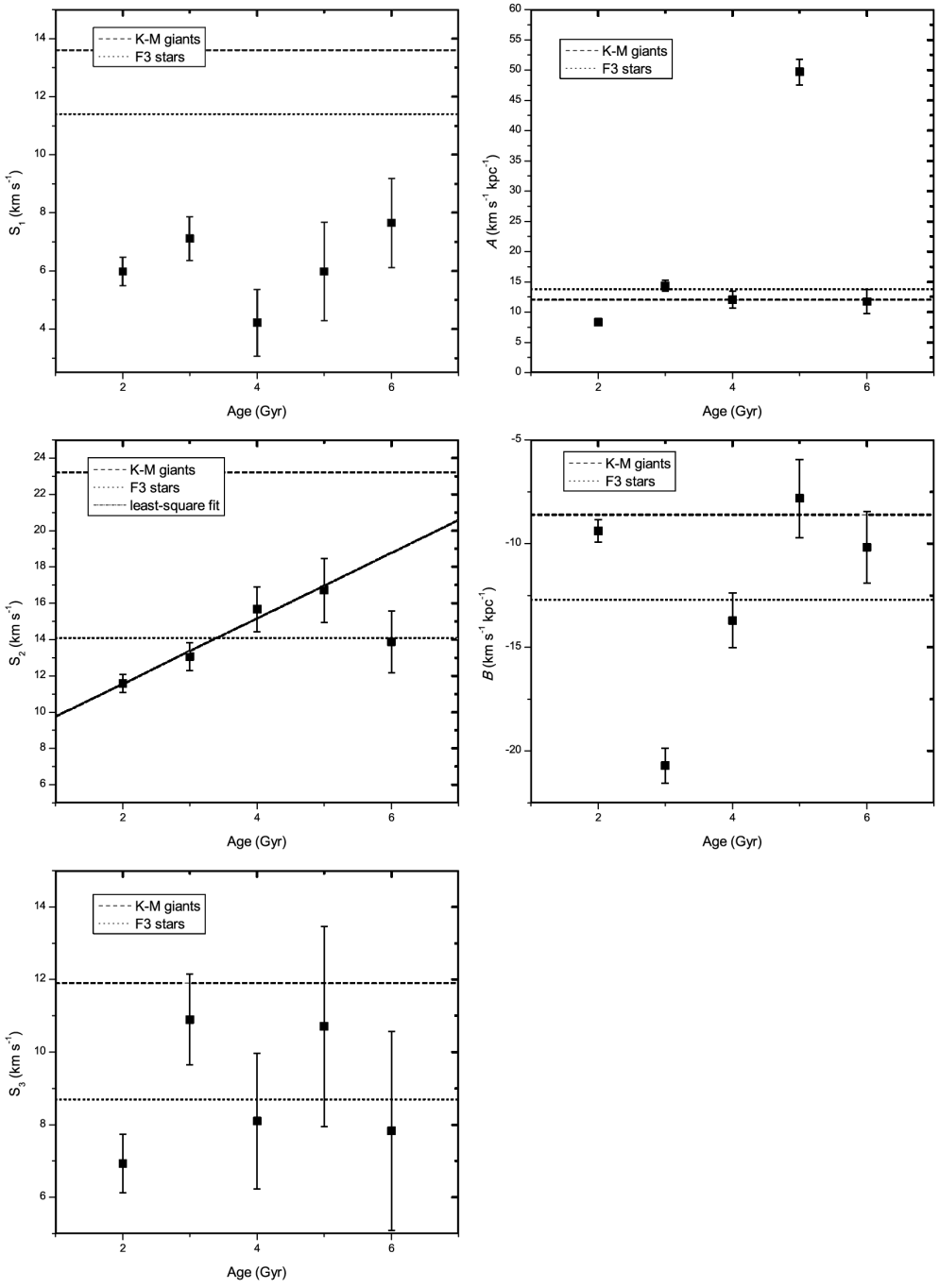

Fig. 4 The age dependence of the kinematical parameters derived from stars in the solar neighborhood. The left three panels are for the solar motions S_1, S_2 and S_3. The right panels are for Oort constants A and B. The dashed line is the value derived from K-M giants, the dotted line is the value derived from F3 stars (Miyamoto & Soma 1993) and the short dash-dotted line is the linear fit of S_2 versus age.

Table 4 Kinematical parameters in different metallicity bins for selected F-type and G-type stars in the ACAD catalog. The parameters derived from the K-M giants and F3-type stars are also listed for comparison.

	Unit	Min in all metallicity bins	Max in all metallicity bins	K-M giants	F3 stars
S_1		5.2 ± 1.0	8.6 ± 1.3	13.6 ± 0.3	11.4 ± 0.7
S_2	($\mathrm{km\,s^{-1}}$)	10.8 ± 1.1	19.7 ± 1.3	23.2 ± 0.3	14.1 ± 0.7
S_3		6.2 ± 0.8	9.5 ± 2.1	11.9 ± 0.3	8.7 ± 0.2
A	($\mathrm{km\,s^{-1}\,kpc^{-1}}$)	2.3 ± 1.2	17.7 ± 0.7	12.0 ± 0.6	13.8 ± 3.5
B		-19.7 ± 0.6	-4.0 ± 1.4	-8.6 ± 0.5	-12.7 ± 2.6

Notes: The K-M giants are distributed from 0.5 kpc to 1 kpc. F3-type stars are distributed from 0.1 kpc to 1.3 kpc (Miyamoto & Soma 1993).

licity, since the distribution of stars is centered at 0 [Sun], the very metal-poor and metal-rich populations are insufficient and would lead to a relatively large error in their kinematical parameters. It is easy to see that the errors of various parameters in metallicity bin $[-0.6, -0.4)$ are two or three times larger than those in other metallicity bins due to an insufficient number of stars. Therefore, the results in this bin have been excluded; the remaining results are listed in Table 4.

We plot variations in the kinematical parameters against metallicity in Figure 5. A similar linear relation can be found between S_2 and metallicity. There is also a clear linear relation between S_1 and metallicity when ignoring the value in metallicity bin $[-0.6, -0.4)$, which has a large fitting error. The rates of S_1 and S_2 are $0.6\ \mathrm{km\,s^{-1}}/\ 0.1$[Sun] and $1.4\ \mathrm{km\,s^{-1}}/\ 0.1$ [Sun], respectively. By interpolating, we find that $S_1 = 6.7\ \mathrm{km\,s^{-1}}$ and $S_2 = 15.1\ \mathrm{km\,s^{-1}}$ at [Fe/H] = 0 [Sun] (metallicity of the Sun).

Schönrich & Binney (2009a) found that stellar migration is the main mechanism that generates the metallicity gradient in the solar neighborhood. Our results for S_1 and S_2 agree well with the conclusion that radial stellar migration causes both non-circular orbits and shifts in the guiding center (Sellwood & Binney 2002). Since the total solar motion ($S_\odot$) can reflect the degree of asymmetric drifts, our results also demonstrate that asymmetric drifts are stronger for the metal-rich populations in Figure 6 (Schönrich et al. 2010). In the figure, $S_\odot$ increases from 14.3 ± 6.3 to $23.5 \pm 2.8\ \mathrm{km\,s^{-1}}$ with respect to metallicity. Nevertheless, $S_\odot$ does not show a clear systematical variation with age.

4.3.1 Rotation of the Sun around the Galactic center

The angular velocity of the Sun around the Galactic center can be described by the difference between the Oort constants A and B

$$A - B = M_{12}^{+} - \Omega_3 = \frac{V_\theta}{R} - \frac{1}{R}\frac{\partial V_R}{\partial \theta}\,. \tag{7}$$

If we assume the motions of stars in the solar neighborhood are circular, we can obtain $\partial V_R/\partial\theta \simeq 0$ and $A - B = V_\theta/R$.

Figure 7 shows the variation of $A - B$ with respect to the metallicity (left panel) and age (right panel), from which no obvious trend can be found. The median values of $A - B$ are 20.7 ± 2.0 and $25.7 \pm 1.9\ \mathrm{km\,s^{-1}\,kpc^{-1}}$ for age and metallicity groupings, respectively. Adopting $R_0 = 8.5\,\mathrm{kpc}$ as the distance from the Sun to the Galactic center, we calculated the rotational velocity of the Sun around the Galactic center with $A - B$ derived from different groups of stars, which gives $V_0 = 175.9 \pm 16.4\ \mathrm{km\,s^{-1}}$ and $V_0 = 218.5 \pm 17.3\ \mathrm{km\,s^{-1}}$ for age and metallicity groupings respectively. The discrepancy in these results between the two kinds of groupings is due to the fact that the age and metallicity are not strictly correlated.

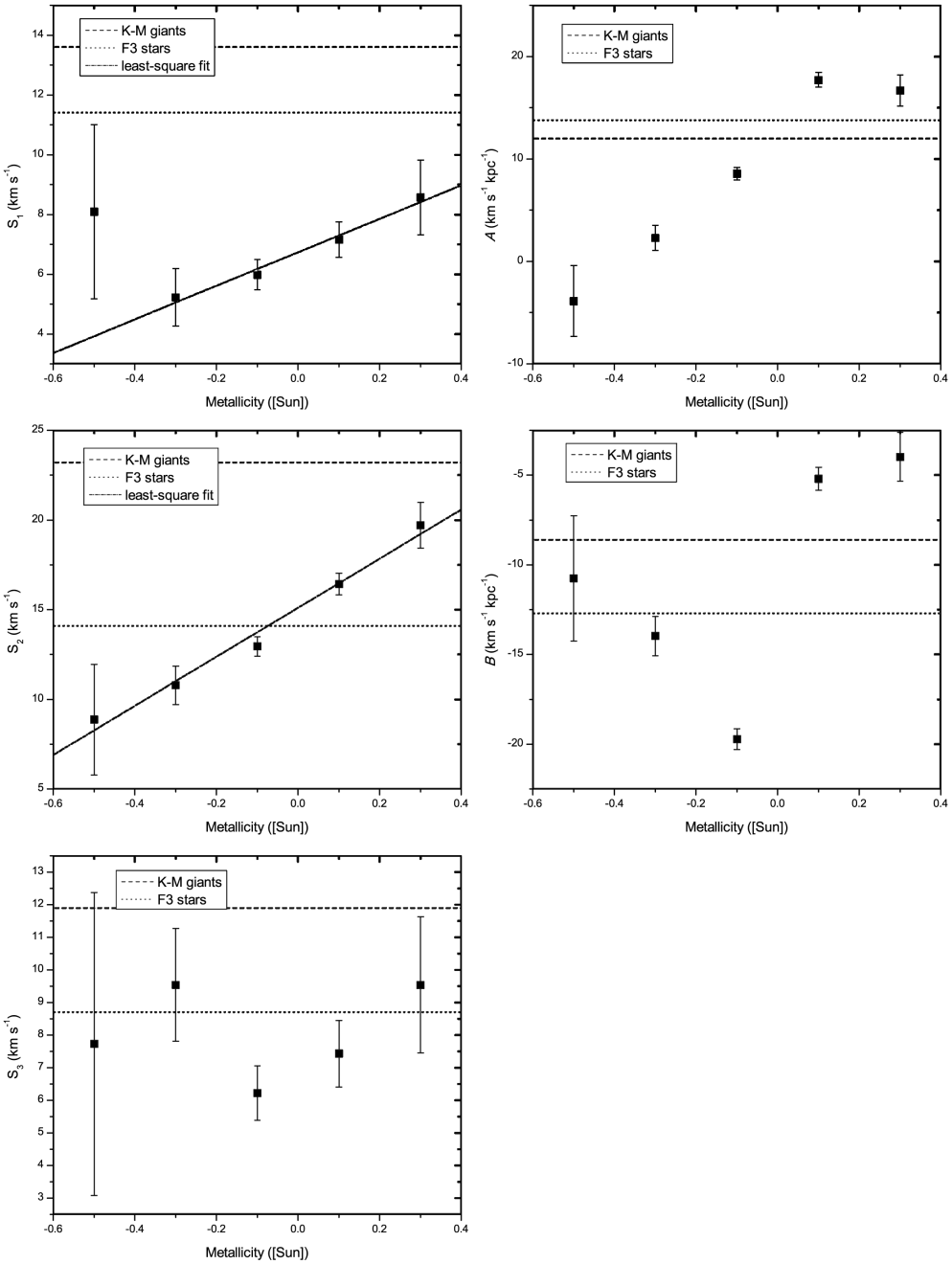

Fig. 5 The metallicity dependence of the kinematical parameters derived from the solar neighborhood stars. The left three panels are for the solar motions S_1, S_2 and S_3. The right two panels are for Oort constants A and B. The dashed line is the value derived from K-M giants and the dotted line is the value derived from F3 stars (Miyamoto & Soma 1993). The short dash-dotted line is the linear fit against metallicity.

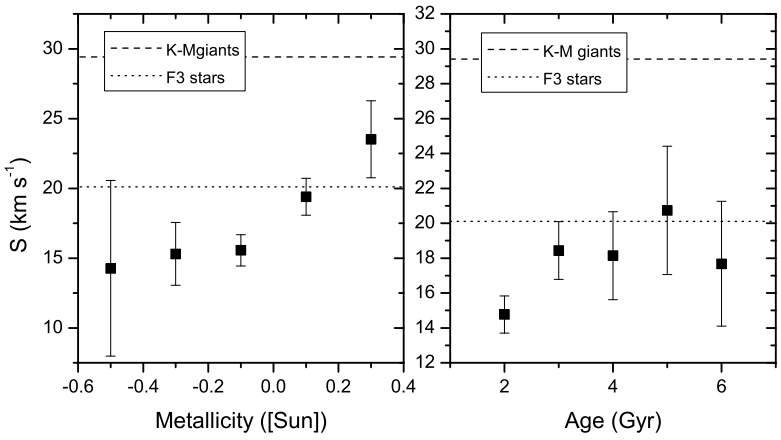

Fig. 6 The total solar motion $S_\odot$ versus age (*right*) and metallicity (*left*). The dashed line is the $S_\odot$ derived from K-M giants and the dotted line is the $S_\odot$ derived from F3-type stars (Miyamoto & Soma 1993).

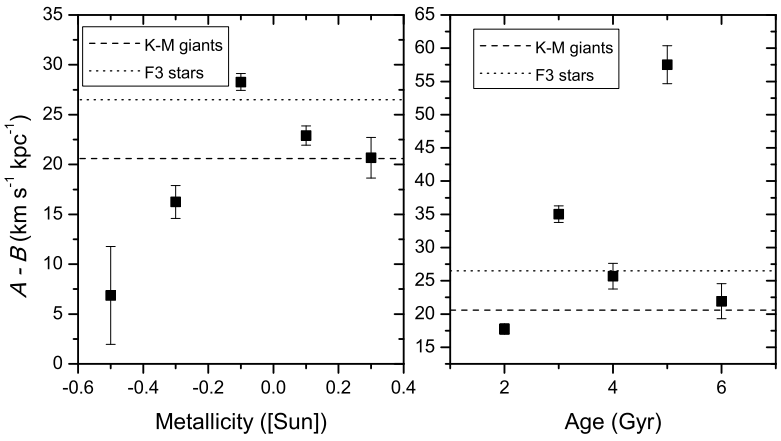

Fig. 7 $A - B$ versus age (*right*) and metallicity (*left*). The dashed line is $A - B$ derived from K-M giants and the dotted line is $A - B$ derived from F3-type stars (Miyamoto & Soma 1993).

5 DISCUSSION AND CONCLUSIONS

In this paper we collected three of the best available catalogs of F-type and G-type stars with astrophysical data. After revising the distance, and supplying radial velocity and photometric data, we built ACAD. It is a comprehensive catalog that incorporates data from eight different catalogs. The total number of stars in ACAD is 27 553. ACAD can be useful for further research on Galactic kinematics. It can also serve as a reference for future astrophysical data. The complete ACAD is available as an electronic table (*http://www.raa-journal.org/raa/index.php/raa/article/view/1715*). Detailed descriptions can be found in Appendix A and Table A.1.

To analyze the kinematics of the stars in the Galactic disk, we used the two-dimensional Lindblad–Oort model to estimate the three-dimensional solar motion and Oort constants A and B. In our study, axisymmetric Galactic potential is no longer a pre-condition and we found that S_2 increases linearly with age which may result from a scattering process. By extrapolating this relationship back to 0 Gyr, S_2 is found to be 8.0 ± 1.2 km s^{-1} for a dynamical cold disk. This value is in the middle of the value ($S_2 = 5.3$ km s^{-1}) calculated by Dehnen & Binney (1998) and the value ($S_2 = 11.0$ km s^{-1}) calculated by Aumer & Binney (2009). It shows that spiral structure still affects the estimation of S_2.

We also found an increase of S_1 and S_2 with respect to metallicity, which indicates that radial stellar migration leads to both non-circular orbits and shifts in the guiding center (Sellwood & Binney 2002). This effect is more significant along the rotational direction ($\mathrm{d}S_2/\mathrm{d}[\mathrm{Fe/H}] = 1.37$ km s^{-1}/0.1[Sun]) than along the radial direction ($\mathrm{d}S_1/\mathrm{d}[\mathrm{Fe/H}] = 0.56$ km s^{-1}/0.1[Sun]). By interpolating, we obtained $S_1 = 6.7$ km s^{-1} and $S_2 = 15.1$ km s^{-1} for stars at solar metallicity.

By using Oort constants A and B, the rotational speed of the Sun around the Galactic center was calculated with different groups of stars. This shows that the LSR which is formed by stars of different ages or metallicities does not systematically affect calculation of the rotational velocity of the Sun.

Before the data release from the next astrometric satellite Gaia, which is expected to provide extremely highly accurate astrometric parameters, radial velocities and photometric data for billions of stars, there is still a gap of more than ten years for us to carry out prospective studies and prepare for future applications of Gaia data. We will update ACAD after collecting more radial velocity, age and metallicity data in the future.

Acknowledgements This work was funded by the National Natural Science Foundation of China (Grant No.11173014) and by the Natural Science Foundation of Jiangsu Province under No. SBK201341200.

Appendix A: DATA DESCRIPTION OF ACAD

The detailed data arrangement of the compiled catalog ACAD is given in Table A.1.

The epoch of the catalog is J2000.0 (ICRS). Explanation for several indexes in ACAD are provided:

(1) FD [F, P, T] represents the distances calculated from different methods:
   F: Fitting distance calculated from proper motion and color.
   T: Parallax distance calculated from trigonometric parallax.
   P: Photometric distance calculated from absolute magnitude and visual magnitude.
(2) FA [1, 3] represents the different sources of astrophysical data:
   1: The Geneva-Copenhagen survey of the solar neighborhood (GCS, Nordström et al. 2004).
   2: The catalog of ages, metallicities, orbital elements and other parameters for nearby F stars (MS95, Marsakov & Shevelev 1995).
   3: The N2K Consortium IV including new temperatures and metallicities for more than 100 000 FGK dwarfs (AM06, Ammons et al. 2006).
(3) FV[1–6] (flag of space velocity) represents the different combinations of proper motion and radial velocity; all the possibilities are listed in Table 1.

Table A.1 Contents of ACAD

No.	Label	Unit	Description
1	GLON	Deg	Galactic longitude
2	GLAT	Deg	Galactic latitude
3	MV	mag	Absolute magnitude
4	DIST	pc	Heliocentric distance of the star
5	UDIST	pc	?=99999.999 Upper confidence limit on heliocentric distance
6	LDIST	pc	?=99999.999 Lower confidence limit on heliocentric distance
7	FD	—	[F, P, T] Flag of distance
8	AGE	Gyr	?=99.99 Age
9	UAGE	Gyr	?=99.99 Upper confidence limit on age
10	LAGE	Gyr	?=99.99 Lower confidence limit on age
11	FE/H	[Sun]	Metallicity
12	UFE/H	[Sun]	?=999.999 Upper confidence limit on metallicity
13	LFE/H	[Sun]	?=999.999 Lower confidence limit on metallicity
14	FA	—	[1,3] Flag of astrophysical data
15	U	km s^{-1}	Heliocentric space velocity component in the radial direction
16	V	km s^{-1}	Heliocentric space velocity component in the direction of rotation
17	W	km s^{-1}	Heliocentric space velocity component perpendicular to the Galactic plane
18	FV	—	[1,6] Flag of space velocity
19	SP	—	?=— Spectral type in MK classification

References

Ammons, S. M., Robinson, S. E., Strader, J., et al. 2006, ApJ, 638, 1004
Aumer, M., & Binney, J. J. 2009, MNRAS, 397, 1286
Barbier-Brossat, M., & Figon, P. 2000, A&AS, 142, 217
Binney, J. 2010, MNRAS, 401, 2318
Bonanno, A., Schlattl, H., & Paternò, L. 2002, A&A, 390, 1115
Casagrande, L., Schönrich, R., Asplund, M., et al. 2011, A&A, 530, A138
Crawford, D. L. 1975, AJ, 80, 955
Dehnen, W., & Binney, J. J. 1998, MNRAS, 298, 387
Edvardsson, B., Andersen, J., Gustafsson, B., et al. 1993, A&A, 275, 101
Famaey, B., Jorissen, A., Luri, X., et al. 2005, A&A, 430, 165
Gontcharov, G. A. 2006, Astronomy Letters, 32, 759
Høg, E., Fabricius, C., Makarov, V. V., et al. 2000, A&A, 355, L27
Holmberg, J., Nordström, B., & Andersen, J. 2009, A&A, 501, 941
Jenkins, A. 1992, MNRAS, 257, 620
Marsakov, V. A., & Shevelev, Y. G. 1995, Bulletin d'Information du Centre de Donnees Stellaires, 47, 13
Miyamoto, M., & Soma, M. 1993, AJ, 105, 691
Nordström, B., Mayor, M., Andersen, J., et al. 2004, A&A, 418, 989
Olsen, E. H. 1984, A&AS, 57, 443
Schönrich, R., & Binney, J. 2009a, MNRAS, 396, 203
Schönrich, R., & Binney, J. 2009b, MNRAS, 399, 1145
Schönrich, R., Binney, J., & Dehnen, W. 2010, MNRAS, 403, 1829
Sellwood, J. A., & Binney, J. J. 2002, MNRAS, 336, 785
Siebert, A., Williams, M. E. K., Siviero, A., et al. 2011, AJ, 141, 187
Steinmetz, M., Zwitter, T., Siebert, A., et al. 2006, AJ, 132, 1645
Wright, C. O., Egan, M. P., Kraemer, K. E., & Price, S. D. 2003, AJ, 125, 359
Zhu, Z. 2000, Ap&SS, 271, 353